Understanding the origin of the S-curve in conjugated polymer/fullerene photovoltaics from drift-diffusion simulations

B. Y. Finck and B. J. Schwartz
Department of Chemistry and Biochemistry, University of California, Los Angeles, Los Angeles, California 90095-1569, USA

(Received 16 May 2013; accepted 12 July 2013; published online 2 August 2013)

We utilize drift-diffusion modeling to investigate the cause of S-shaped current-voltage curves in organic solar cells. We find that even a many order-of-magnitude mismatch of the carrier mobilities is insufficient to generate S-shaped J-V curves. Instead, S-shaped J-V curves result when a sigmoid-shaped electron mobility profile is entered into the calculation. This suggests that S-curves in bulk heterojunction photovoltaics are caused by factors that affect the extraction of electrons near the device cathode. Such factors could include surface recombination, partially blocking contacts caused by interfacial layers, or vertical phase separation of the fullerenes away from the cathode interface. © *2013 AIP Publishing LLC*. [http://dx.doi.org/10.1063/1.4817396]

Organic solar cells have emerged as a potentially viable source of renewable energy, with power conversion efficiencies (PCEs) reported to be as high as 10%. Unfortunately, it is difficult to maintain such high efficiencies when scaling organic photovoltaics (OPVs) from laboratory scales to mass production because the nanometer-scale morphology of the bulk heterojunction (BHJ) active layer depends sensitively on the kinetics of how the films are processed. This sensitivity to processing kinetics is so extreme that it is often difficult to reproducibly obtain PCEs for a given set of materials from day to day. As an example of this lack of reproducibility, organic solar cells sometimes exhibit an S-shaped current-voltage curve, resulting in low PCE because of a significantly reduced fill factor (*FF*), even if the short circuit current (J_{sc}) and open circuit voltage (V_{OC}) remain high. Thus, understanding the cause of S-shaped *J–V* curves would help to allow for the rational design of OPV devices, thus improving their reproducibility and potential industrial feasibility.

Several groups have proposed hypotheses to explain the appearance of S-shaped *J-V* curves in OPVs. Early work suggested that the problem involved diminished electron extraction due to defects at the cathode interface.[1,2] Others have argued that an imbalance of the individual charge carrier mobilities would induce S-shaped *J–V* curves, and this has been demonstrated for planar junctions (bilayer solar cells).[3] This explanation does not appear to extend to typical BHJ devices, however, since organic donor/acceptor blends often have uneven hole and electron mobilities, which would mean that S-shaped *J-V* curves would be more common if charge mobility imbalance alone was the primary culprit. We previously have argued that S-shaped *J-V* curves in OPVs result from vertical phase separation of the two organic components,[4] for example, when the fullerenes that carry the electron current sink towards the bottom contact and away from the cathode. Our evidence included surface topographic measurements that indicated that the interface between the active layer and the cathode in S-curve devices was deficient in fullerene, that S-curve devices had a 'double peak' in the current extracted in photo-CELIV experiments, and that the S-curve could be subsequently removed if additional fullerene was deposited on the top surface before application of the cathode contact.[4]

In this letter, we utilize drift-diffusion modeling to investigate the cause of S-shaped *J-V* curves in BHJ organic solar cells. We take advantage of the approach of Häusermann *et al*. to simulate OPVs, approximating the BHJ as a 1-D device treated as an effectively uniform medium.[5] We used the Gummel method[6] to decouple the charge carrier continuity and Poisson equations which make up the drift-diffusion model and assumed thermionic injection at the contacts as boundary conditions for the electron and hole densities.[7] In order to account for thin-film interference effects, we used the Petterson transfer matrix method[8] to calculate the spatially dependent absorption profile that determines the initial generation of charge carriers for the continuity equations. For this calculation, we assumed that the active layer had the optical characteristics of poly-3-hexylthiophene (P3HT) and that every exciton immediately splits into an electron and a hole (an assumption justified by the fact that the exciton diffusion length in P3HT is thought to be small compared to the spatial variation of the carrier generation profile).[9] Finally, we also assumed a bimolecular Langevin mechanism[10] to account for the recombination of electrons and holes. All the pertinent parameters for our simulations are collected in Table I.

We began by testing the supposition that imbalanced charge extraction rates as a result of a carrier mobility mismatch might be responsible for the appearance of S-shaped *J-V* curves in BHJ devices. We simulated the *J-V* characteristics of a series of BHJs with increasingly mismatched carrier mobilities. Our initial calculation assumed matched electron and hole mobilities with a numerical value of 1×10^{-4} cm^2/Vs. We then decreased the electron mobility by over 5 orders of magnitude, producing the *J-V* characteristics shown in Fig. 1(a). Our calculations plainly show that although mismatched carrier mobilities can significantly reduce the PCE and FF of BHJ solar cells, mismatched carrier mobilities alone are not responsible for the characteristic S-shaped *J-V* curve, in line with our arguments above.

We next investigated the hypothesis that difficulty with extraction of one of the carriers at a contact is responsible

TABLE I. The parameters used for the simulations presented in the figures, except where otherwise noted.

Parameter	Symbol	Numerical value
Hole mobility	μ_P	1×10^{-4} cm V^{-1} s^{-1}
Electron mobility before drop-off	μ_{n0}	1×10^{-4} cm V^{-1} s^{-1}
Electron mobility after drop-off	y	1×10^{-6} cm V^{-1} s^{-1}
Abruptness of drop-off	σ	1.0
Distance of drop-off from cathode contact	X	20 nm
Thickness	d	100 nm
Relative permittivity	ε	3.5
Injection barrier for electrons and holes	φ_n,φ_p	0.3 eV
Recombination efficiency	η	0.5
Built in voltage	V_{BI}	0.6 V
Density of chargeable sites	N_C	1×10^{26} m^{-3}
Temperature	T	298 K

for the appearance of S-shaped J-V curves. To simulate the effects of poor electron extraction near the cathode, we modeled the spatial mobility profile of the electrons $\mu_n(x)$ using a sigmoid function

$$\mu_n(x) = \frac{\mu_{n0}}{1 + \exp\Big(\sigma(x - X)\Big)} + y. \quad (1)$$

Such a function results in a smooth drop-off in electron mobility in one region of the active layer. In this sigmoid function, σ and X control the sharpness and position of the mobility drop-off, respectively, while y represents for the non-zero mobility of electrons in P3HT as they are extracted from the cathode; for y, vertical phase separation characterized by fullerenes drifting away from the cathode, an interfacial extraction barrier, "blocking contact," or surface recombination all could cause this mobility to be up to several orders of magnitude less than μ_{n0}, the electron mobility in the region before the drop-off. We chose to leave the hole mobility constant in this region and throughout the device.

There are three parameters in the mobility profile of Eq. (1) that could potentially influence the character of the resulting simulated J-V curve: the position within the device where the mobility drop-off begins (X), the mobility of the carrier beyond the drop-off point (y), and the steepness of the drop-off (σ). We explore the effects of varying each of these parameters on the device J-V curves in Figs. 1(b)–1(d);

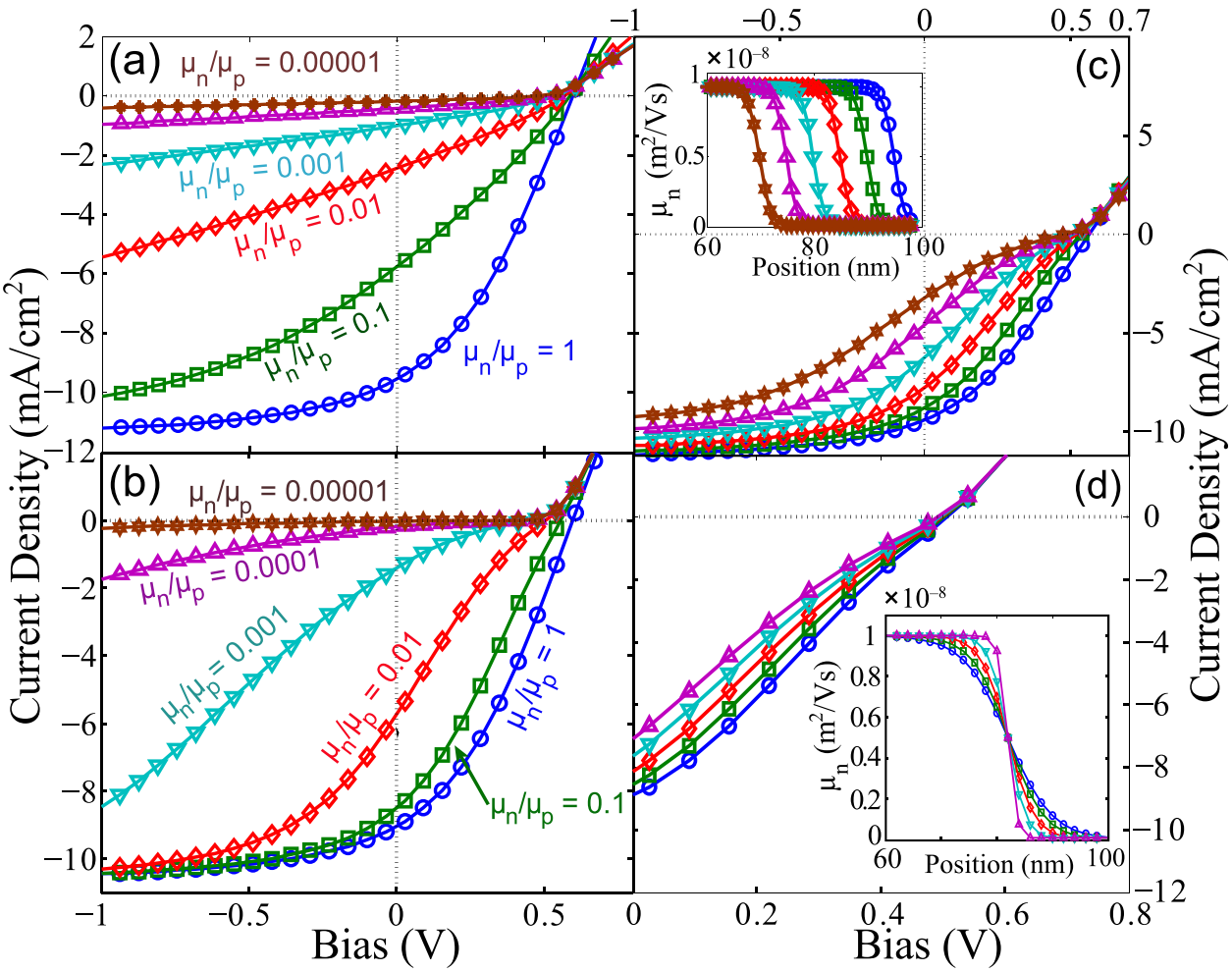

FIG. 1. Simulated J-V curves analyzed in this study. The electron and hole mobilities are initially equalized to 1×10^{-4} cm^2/Vs. The electron mobility is subsequently reduced by several orders of magnitude in two manners: (a) by decreasing the electron mobility throughout the device and (b) by only decreasing the mobility only near the cathode through the use of a sigmoid profile. Fig. 1(a) illustrates the inability of mismatched carrier mobilities to induce an S-curve; Fig. 1(b) illustrates that a sigmoid-shaped electron mobility profile is capable of inducing an S-curve. The effects of the different features of the mobility profile are explored by increasing the size (c) and abruptness (d) of the mobility drop-off, as illustrated in the insets over an expanded spatial region of the 100-nm thick device active layer. Increasing the region of reduced mobility and the abruptness of the drop in mobility results in a more pronounced S-curve character.

the insets show the mobility profiles used for each *J-V* curve. Since Fig. 1(a) can be compared directly to Fig. 1(b) in terms of the effective reduced carrier mobility at the cathode contact, our simulations clearly show that it is not reduced carrier mobility alone but rather the presence of a mobility drop-off (even a relatively small one) that is responsible for producing S-shaped *J-V* curves in, otherwise, normal BHJ devices. Of particular note is that the S-curve appears when the mobility in the drop-off region is 2 orders of magnitude less for electrons than for holes.

To understand why a mobility drop-off leads to S-shaped *J*-V curves, we examined the individual (but spatially averaged throughout the device) carrier current densities as a function of the applied voltage, as shown in Fig. 2. Even though the hole current exhibits typical diodic behavior (albeit with slightly reduced efficiency), Fig. 2 illustrates that the presence of the mobility drop-off for the electrons leads to an electron current with a significant S-shaped character and reduced V_{OC}. Since the total current density is a sum of the individual carrier current densities, the result is a device *J-V* curve with pronounced S-shaped character. This is in contrast to a normal BHJ device (also plotted in Fig. 2), in which both carrier currents exhibit typical diodic behavior.

The cause of the reduction in the spatially averaged current can be further understood by examining the spatial dependence of the current densities at key points along the *J-V* curve for devices with and without the electron mobility drop-off, as shown in Figure 3. At short-circuit conditions, Fig. 3(a) shows that the total current is limited by the electron current near the cathode contact. Photogenerated electrons drift towards the cathode until they reach the low mobility region, where they slow to a constant and relatively slow speed. The hole current is also limited in this region, but this does not have an appreciable effect on the total current since the hole density (and thus hole current) is typically low here under short circuit conditions. As the voltage is

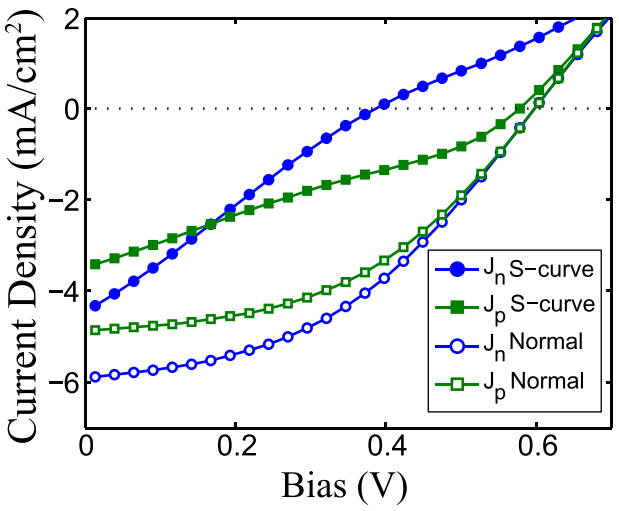

FIG. 2. Individual charge carrier currents for S-curve (solid symbols, device parameters given in Table I) and normal OPV (open symbols, no mobility drop-off) devices. The normal device shows typical *J-V* diodic behavior for the individual carriers, but the device with the mobility drop-off has a severely distorted *J-V* character, particularly for the electron current (blue curves).

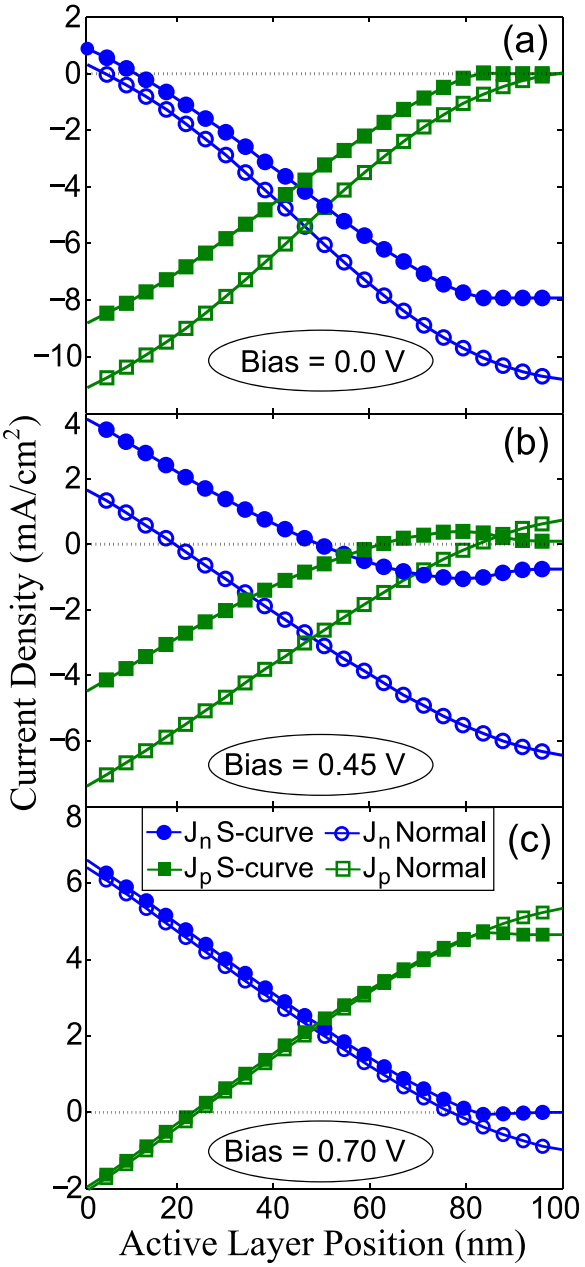

FIG. 3. Spatially discretized electron current (J_n) and hole current (J_p) at various applied voltages for both an S-curve device (solid symbols, parameters given in Table I) and a normal BHJ device (open symbols, no mobility drop-off). The currents are shown at applied voltages corresponding to (a) short circuit conditions, (b) near the inflection point of the *J-V* curve, and (c) beyond V_{OC}. In panel (b), there is severe distortion of the individual carrier currents for the S-curve device, which results in a reduced total current and an inversion of the current gradients, resulting in a buildup of charge. At higher biases, the severity of this inversion is reduced, and normal behavior is re-established.

increased, Fig. 3(b) shows that the electron and hole currents gain a positive and negative slope, respectively. According to the current gradient term in the continuity equation, this reverse in slope results in a buildup of space charge near the cathode, explaining why the electron current becomes limited at this voltage. At higher applied biases (V_{OC} and beyond), this gradient inversion is diminished, and the *J-V* characteristic behaves as a normal OPV device as the charge carriers begin moving towards their reverse contacts. In this case, electron transport is no longer hampered by the

mobility drop-off as the electrons are extracted through the anode instead of the cathode. Similarly, hole extraction is not restricted at the cathode since hole mobility is kept at sufficiently high in the pure P3HT there, in accordance with the phenomenon of vertical phase segregation. Taken together, this explains why the electron current has such a strong S-shape: the electron current becomes limited at intermediate voltages where there is significant space-charge build-up but then approaches "normal" values once V_{OC} is exceeded.

In summary, we have shown that a simple mobility profile characterized by drop in conductivity near one of the contacts is sufficient to induce an S-shaped J-V curve in a simulated organic photovoltaic device. Such a mobility profile, in which there is an imbalance in carrier mobility at only one of the contacts, would certainly arise as a result of vertical phase segregation, a "blocking contact" or other interfacial effects. The results are consistent with our earlier suggestion that subtleties in processing conditions that produce vertical phase segregation are a likely culprit for the appearance of S-curves in BHJ devices.[5] Thus, to avoid irreproducibility in device performance from changes in processing conditions, it would make sense to employ techniques that are less susceptible to kinetics, such as sequential deposition of the donor and acceptor materials.[11]

[1]D. Gupta, M. Bag, and K. S. Narayan, Appl. Phys. Lett. **92**, 093301 (2008).
[2]M. Glatthaar, M. Riede, N. Keegan, K. Sylvester-Hvid, B. Zimmermann, M. Niggemann, A. Hinsch, and A. Gombert, Sol. Energy Mater. Sol. Cells **91**, 390–393 (2007).
[3]W. Tress, A. Petrich, M. Hummert, M. Hein, K. Leo, and M. Riede, Appl. Phys. Lett. **98**, 063301 (2011).
[4]B. T. de Villers, C. J. Tassone, S. H. Tolbert, and B. J. Schwartz, J. Phys. Chem. C **113**(44), 18978–18982 (2009).
[5]R. Häusermann, E. Knapp, M. Moos, N. A. Reinke, T. Flatz, and B. Ruhstaller, J. Appl. Phys. **106**, 104507 (2009).
[6]H. Gummel, IEEE Trans. Electron Devices **11**, 455 (1964).
[7]J. C. Scott and G. G. Malliaras, Chem. Phys. Lett. **299**, 115 (1999).
[8]L. A. A. Pettersson, L. S. Roman, and O. Inganas, J. Appl. Phys. **86**, 487 (1999).
[9]J. Guo, H. Okhita, H. Benten, and S. Ito, J. Am Chem. Soc. **132**, 6154 (2010).
[10]L. J. A. Koster, V. D. Mihailetchi, and P. W. M. Blom, Appl. Phys. Lett. **88**, 052104 (2006).
[11]A. L. Ayzner, C. J. Tassone, S. H. Tolbert, and B. J. Schwartz, J. Phys. Chem. C **113**, 20050 (2009).